

## Three-Site Model for Hydrogen Adsorption on Supported Platinum Particles: Influence of Support Ionicity and Particle Size on the Hydrogen Coverage

Michiel K. Oudenhuijzen, Jeroen A. van Bokhoven,<sup>†</sup> Jeffrey T. Miller,<sup>‡</sup>  
David E. Ramaker,<sup>§</sup> and Diederik C. Koningsberger\*

*Contribution from the Department of Inorganic Chemistry and Catalysis, Debye Institute, Utrecht University, PO Box 80083, 3508 TB Utrecht, The Netherlands, BP Amoco Chemicals Research Center, Mail Station E-1F, 150 West Warrenville Road, Naperville, Illinois 60563-8460, and the Chemistry Department, George Washington University, Washington, D.C. 20052*

Received August 11, 2004; E-mail: d.c.koningsberger@chem.uu.nl

**Abstract:** Pt L<sub>3</sub> X-ray absorption edge data on small supported Pt particles ( $N < 6.5$ ) reveals that at very low H<sub>2</sub> pressure or high temperature the strongest bonded H is chemisorbed in an atop position. With decreasing temperature or at higher H<sub>2</sub> pressure only  $n$ -fold ( $n = 2$  or  $3$ ) sites are occupied. At high H<sub>2</sub> pressure or low temperature, the weakest bonded H is positioned in an "ontop" site, with the chemisorbing Pt already having a stronger bond to a H atom in an  $n$ -fold site. DFT calculations show that the adsorption energy of hydrogen increases for Pt particles on ionic (basic) supports. The combination of the DFT calculations with hydrogen chemisorption data and the analysis of the Pt L<sub>3</sub> X-ray absorption spectra implies that both the H coverage and/or the type of active Pt surface sites, which are present at high temperature catalytic reaction conditions, strongly depend on the ionicity of the support. The consequences for Pt catalyzed hydrogenolysis and hydrogenation reactions will be discussed.

### Introduction

H adsorption on supported Pt particles is critical in supported noble metal catalysts, which are widely used in commercially important reactions, including hydrogenation, naphtha reforming, isomerization reactions, and in electrocatalysis such as that taking place in a fuel cell.<sup>1</sup> Recent advances<sup>2,3,4</sup> in the analysis procedures of the Pt L<sub>3</sub> and L<sub>2</sub> X-ray absorption near edge spectra (XANES) provide H binding site information in situ on supported Pt particles both in the gas phase and in an electrochemical cell. The Pt L<sub>3</sub> XANES data of the clean sample (when the Pt surface is free of H) is subtracted from the data obtained after chemisorption of hydrogen:  $\Delta\mu_{L3} = \mu_{L3}(H/Pt) - \mu_{L3}(Pt)$ . As shown by theoretical data obtained with the help of full multiple scattering ab initio calculations using the FEFF8 code, the signature of this difference spectrum ( $\Delta\mu_{L3}$ ) is characteristic for a particular geometry of the Pt–H binding site.

For large ( $N_{Pt} > 9$ , 2–3 nm) Pt particles supported on carbon, Teliska et al.<sup>4</sup> found, using this XANES  $\Delta\mu$  method in

an electrochemical cell on a Pt/C electrode, strong evidence for delocalized H (relatively fast H hopping from fcc via the bridged to hcp sites and returning) on the surface at low coverage (around 0.3 V RHE). As the coverage increases H is found in  $n$ -fold sites. When the potential moves down still further to 0.0 V RHE leading to an even higher coverage, H can absorb on top of a Pt surface atom, which already has a stronger bond to a H atom in a 3-fold site. This H will be further referred to as "ontop" H in this work. These authors distinguished 5 different features in the H TPD curves for polycrystalline Pt, and 5 related features in the CV curves in an electrochemical cell. These features correspond to the following three types of adsorption sites, in order of increasing adsorption bond strength,  $\Delta H$ : (i) ontop H near edges, (ii) 3-fold H and delocalized H on faces, (iii) 3-fold H and delocalized H near edges. Figure 1(left side) summarizes the TPD results for these 5 different sites present on polycrystalline Pt with the temperature scale at the left indicating the approximate temperatures of the peaks in the TPD curves. Both the  $\Delta H$  and  $\Delta S$  for adsorption of H in the primary two absorption sites (3-fold on faces: 3-f<sub>f</sub> and near edges: 3-f<sub>e</sub>) existing for H/Pt in an electrochemical environment have been obtained from the CV curves. The  $\Delta H$  values obtained from these studies are comparable to those obtained in the gas phase and from theoretical calculations<sup>5</sup> suggesting strongly that the H binding sites in the electrolyte and gas phase are comparable.

(3) Koningsberger, D. C.; Oudenhuijzen, M. K.; de Graaf, J.; van Bokhoven, J. A.; Ramaker, D. E. *J. Catalysis* **2003**, *216*, 178–191.

(4) Teliska, M.; O'Grady, W. E.; Ramaker, D. E. *J. Phys. Chem. B* **2004**, *108*, 2333–2344.

\* To whom correspondence should be addressed. Laboratory of Inorganic Chemistry and Catalysis, Debye Institute, Utrecht University, P.O. Box 80083, 3508 TB, The Netherlands. Tel: +31302573400. E-mail: d.c.koningsberger@chem.uu.nl.

<sup>†</sup> Present address: ETH Zürich, HCI E115, 8093 Zürich, Switzerland.

<sup>‡</sup> BP Amoco Chemical Research Center.

<sup>§</sup> George Washington University.

(1) Gates, B. C. *Chem. Rev.* **1995**, *95*, 511–522.

(2) Ramaker, D. E.; Koningsberger, D. C. *Phys. Rev. Lett.* **2002**, *89*, 139701–139702.

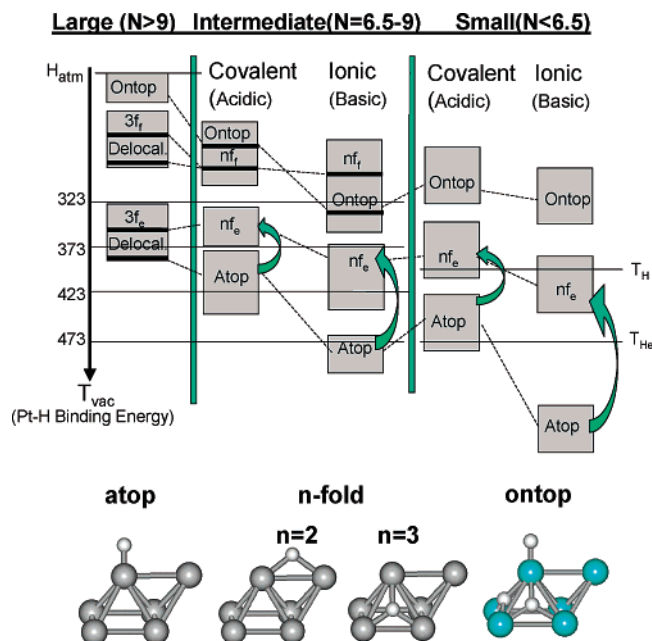


**Figure 1.** Temperature ranges of TPD hydrogen desorption for the different hydrogen binding sites at approximately  $10^{-4}$  to  $10^{-6}$  Torr. For an atop site H is bonded to only one Pt, which has no bonds to other H atoms. For a 2- or 3-fold site H is bonded to 2 or 3 Pt atoms, which also have no bonds to other H atoms. A 3-fold hydrogen is sitting in the triangular surface plane. ( $nf_e$ :  $n$ -fold Pt edge site;  $nf_f$ :  $n$ -fold Pt face site with  $n = 2$  or 3). For an ontop site H is bonded to only one Pt, which already has bonds to other H atoms.

In an earlier paper,<sup>6</sup> we focused on elucidating the nature of the adsorbed H found at different temperatures in the gas phase, namely in understanding the common  $H_2$  chemisorption conditions that routinely exist when determining the dispersion of supported metal particles.<sup>7</sup> In such  $H_2$  chemisorption (H/M) experiments, H is adsorbed at the metal surface at room temperature, giving the so-called first isotherm of H chemisorption. After evacuation at room temperature, a second isotherm is commonly measured. The H that gives rise to the second isotherm is normally called “reversibly” adsorbed H, since it can adsorb and desorb after evacuation at RT. The amount of “irreversibly” adsorbed H is determined by the difference between the first and the second isotherm. Using XANES data from a basic Pt/K- $Al_2O_3$  catalysts with Pt–Pt coordination number around 6.5, it was shown that both types of H are indeed atomically chemisorbed on the metal surface of a supported Pt catalyst.

There are strong indications that the ionicity of the support influences the electronic structure of the supported Pt particles.<sup>8,9</sup> The influence of the support ionicity on the chemisorption properties of H on small (less than 1.2 nm:  $N_{Pt-Pt} < 6.5$ ; right side of Figure 1) Pt particles dispersed in LTL and Y zeolite has been studied in detail by our group using the new XANES  $\Delta\mu$  analysis procedure as described above.<sup>3</sup> H was found in the Pt  $n$ -fold ( $n = 2$  or 3) sites for Pt particles on ionic supports

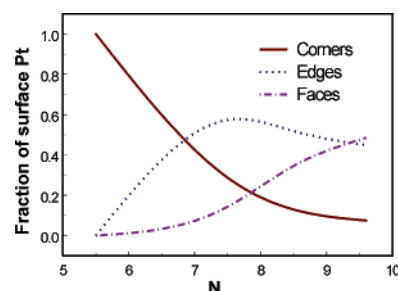


**Figure 2.** Fraction of corner, 3-fold edge and 3-fold face Pt surface sites as a function of the Pt–Pt first shell coordination number  $N$ .

(or basic, with electron rich support oxygen atoms), while on covalent (or acidic, with electron poor oxygen atoms) supports the H was found in the atop sites under the specific conditions utilized in that work. This was the first spectroscopic in situ observation of chemisorbed H in an atop site on the surface of small supported Pt particles. DFT calculations<sup>3,10</sup> show that the Pt  $sp$  orbitals are important for H bonding, and that the rearrangement of the Pt  $6s, 6p$  interstitial bond orbitals (IBO) instigated by the support ionicity leads to a larger Pt–H bond strength on ionic supports. The consequence of these findings is that the H coverage is larger on Pt particles dispersed on ionic supports.

Although we have identified 3 types (and even 5 different sites) of adsorbed H above, the TPD and electrochemical data for polycrystalline Pt reveal just two dominant features. It is natural to relate these two features to the chemisorption results, which distinguishes between weakly and strongly bonded H as discussed above. On the basis of Figure 1, one could conclude in general that both the “reversibly” (weakly) and “irreversibly” (strongly) chemisorbed H is bonded in the  $n$ -fold sites, the weaker to  $n$ -fold sites on the faces, and the stronger to  $n$ -fold sites near the edges. However, for very small particles ( $N < 6.5$ , less than 1.0 nm), flat faces are absent, yet the TPD curves still show two primary (and even more) features.<sup>11</sup> It is possible that now so-called ‘weakly’ adsorbed H is bonded in the ontop sites and the ‘strongly’ adsorbed H in the  $n$ -fold sites. For intermediate sized particles ( $6.5 < N < 9$ ) corners, edges as well as faces exist on the clusters<sup>12</sup> (see Figure 2) making the situation even more complicated. Thus it is not immediately clear which H is weakly and strongly adsorbed in all cases.

In this paper, a three-site adsorption model (see Figure 1) is proposed for H adsorption on small and intermediate Pt particles. Pt  $L_{3\text{ edge}}$  XANES data using the above-mentioned  $\Delta\mu$  signatures is used to examine Pt/ $Al_2O_3$ , having intermediate size Pt particles. The XANES results show the presence of atop H at low coverage and ontop hydrogen at high coverage. DFT calculations elucidate that due to lateral interactions the strongest bonded atop hydrogen existing at low coverage moves to the  $n$ -fold sites with increasing coverage. This allows these atop sites to be refilled at higher coverage, leading to the weakest bonded ontop hydrogen. Therefore, the Pt–H bond strength increases in the order ontop  $<$   $n$ -fold  $<$  atop. The XANES  $\Delta\mu$  data and the results of the DFT calculations suggest that the

(5) Kua, J.; Goddard, W. A. *J. Phys. Chem. B* **1998**, 102 (47), 9481–9491.  
 (6) Oudenhuijzen, M. K.; Bitter, J. H.; Koningsberger, D. C. *J. Phys. Chem. B* **2001**, 105, 4616–4622.  
 (7) Scholten, J. J. F.; Pijpers, A. P.; Hustings, A. M. L. *Catal. Rev.—Sci. Eng.* **1985**, 27, 151–206.  
 (8) Mojet, B. L.; Miller, J. T.; Ramaker, D. E.; and Koningsberger, D. C. *J. Catal.* **1999**, 186, 373–386.  
 (9) Ramaker, D. E.; de Graaf, J.; van Veen, J. A. R.; Koningsberger, D. C. *J. Catal.* **2001**, 203, 7–17.

(10) Oudenhuijzen, M. K.; van Bokhoven, J. A.; Ramaker, D. E.; Koningsberger, D. C. *J. Phys. Chem. B* **2004**, 108, 20247–20254.  
 (11) Miller, J. T.; Meyers, B. L.; Modica, F. S.; Lane, G. S.; Vaarkamp, M.; Koningsberger, D. C. *J. Catal.* **1993**, 143, 395–408.  
 (12) Gordon, M. B.; Cyrot-Lackmann, F.; Desjonqueres, M. C. *Surf. Sci.* **1977**, 68, 359–367; Benfield, R. E., *J. Chem. Soc., Faraday Trans.* **1992**, 88, 1107–1110.

hydrogen coverage, which would exist on the Pt surface at high temperature catalytic reaction conditions, should strongly depend on the ionicity of the support and the particle size. Since Pt particles on acidic supports are the most active in hydrogenation and hydrogenolysis reactions, it is entirely possible that the difference in catalytic activity is related to differences in H chemisorption properties. Furthermore, the classification of these three sites into weakly and strongly bonded H depends strongly on the ionicity of the support.

## Experimental Section

**Catalyst Preparation.** Details of the preparation are given elsewhere.<sup>8</sup> In summary, the acidity/alkalinity of the LTL zeolite supports was varied by either impregnating a commercial K-LTL zeolite with KNO<sub>3</sub> or exchanging it with NH<sub>4</sub>NO<sub>3</sub> to give K/Al ratios ranging 0.63 to 1.25. Each LTL zeolite was calcined at 500 K. Platinum (1 wt %) was added by incipient wetness impregnation using an aqueous solution of [Pt(NH<sub>3</sub>)<sub>4</sub>](NO<sub>3</sub>)<sub>2</sub> followed by drying at 393 K. The catalysts are designated Pt/LTL(*x*) with *x* representing the K/Al molar ratio.

Two Al<sub>2</sub>O<sub>3</sub> supported Pt catalysts containing 2 wt % Pt were prepared. Details on the loading of the support with Pt are given elsewhere.<sup>6</sup> The support of one of the Pt/Al<sub>2</sub>O<sub>3</sub> catalysts was made alkaline by impregnating it with a KOH solution, yielding a support containing 0.25 wt % K. This catalyst is further referred to as Pt/K–Al<sub>2</sub>O<sub>3</sub>. The support of the second catalyst was made acidic by impregnating it with a HCl solution, resulting in a 3.3 wt % Cl loading. This catalyst is coded Pt/Cl–Al<sub>2</sub>O<sub>3</sub>.

**XAFS Data Collection.** XAFS measurements were performed at the SRS (Daresbury) Wiggler Station 9.2 (Pt/LTL supports) and the European Synchrotron Radiation Facility (Swiss-Norwegian Beamline) in Grenoble, France (Pt/Al<sub>2</sub>O<sub>3</sub> supports). The measurements were done in transmission mode using ion chambers filled with Ar to have an X-ray absorbance of 20% in the first and of 80% in the second ion chamber. The monochromator was detuned to 50% maximum intensity to avoid higher harmonics present in the X-ray beam.

The samples were pressed into a self-supporting wafer (calculated to have an absorbency of 2.5) and placed in a controlled atmosphere cell operated at 1 atm.<sup>13</sup> The Pt/LTL catalysts were reduced in flowing H<sub>2</sub> (5% H<sub>2</sub> in He) at 573 K (termed *T<sub>H</sub>* in this work). The samples were then cooled to liquid nitrogen temperature with the in-situ cell closed and the XAFS spectra were recorded. The reduced catalyst is further denoted as 'RED'. A subsequent treatment in flowing He for 1 h at 573 K (termed *T<sub>He</sub>* in this work) was used to remove part of the chemisorbed hydrogen followed by XAFS experiments in He at liquid nitrogen temperatures<sup>8</sup> 'He573'. Controlled hydrogen adsorption/desorption experiments were carried out for the Al<sub>2</sub>O<sub>3</sub> supported catalysts. The catalysts were first reduced in flowing H<sub>2</sub> at 673 K in situ and cooled in flowing H<sub>2</sub> (5% H<sub>2</sub> in He) to liquid nitrogen (LN) temperature. At this temperature, the XAFS spectra were recorded. This freshly reduced catalyst is further denoted as 'RED'. Next, the catalysts were evacuated at 323, 373, 423, and 473 K for 30 min (all heating rates were 5 K/minute). After the respective evacuations at each temperature, the catalysts were cooled to LN, and the L<sub>2</sub>/L<sub>3</sub> XAFS spectra were collected maintaining a pressure of lower than 10<sup>−3</sup> Pa. These samples are further referred to as 'VAC323', 'VAC373', 'VAC423', and 'VAC473', respectively. Logically, the H coverage increases in the order VAC473 < VAC423 < VAC373 < VAC323 < RED.

**EXAFS Data-Analysis.** The EXAFS data-analysis and the resulting EXAFS coordination parameters of the Pt/LTL samples are given and discussed in an earlier paper.<sup>8</sup> The fits on the EXAFS data of the Al<sub>2</sub>O<sub>3</sub> supported Pt catalysts were performed in *R*-space (*k*<sup>2</sup>, 2.5 < *k* < 14

Å<sup>−1</sup>, 1.6 < *R* < 3.2 Å) using the difference file technique.<sup>14</sup> Using these *k*- and *R*-ranges, the number of independent parameters (*N<sub>ind</sub>*) is calculated to be 13.7. Pt–Pt and Pt–O contributions were used for the fits. Therefore, a fit with 8 free parameters (each coordination shell implies the use of 4 free parameters) had to be applied. The O backscatterer originates from the LTL<sup>15</sup> and the Al<sub>2</sub>O<sub>3</sub><sup>16</sup> supports. Further details of the analysis are given elsewhere.<sup>6</sup>

**Near Edge Analysis of the Pt L<sub>3</sub> X-ray Absorption Edges.** The pre-edge subtracted and normalized XANES spectra for each catalyst after reduction and after the various evacuations were aligned in order to remove initial and final state screening effects.<sup>17</sup> First, the energy of the point in the step edge having an intensity of 0.6 in the normalized L<sub>2</sub> XANES of clean Pt is set to zero. Then the L<sub>2</sub> edges for H/Pt and Pt are aligned. This is followed by aligning the EXAFS structure (both for the H/Pt and Pt data separately) in the L<sub>2</sub> and L<sub>3</sub> spectra in the region between 50 and 120 eV beyond the edge using a least-squares method. At these energies, the contribution to the EXAFS of the H atoms is negligible. Thus, the four spectra (L<sub>2</sub> and L<sub>3</sub> for the Pt and H/Pt) are all consistently aligned for each calculation of Δ*μ<sub>L3</sub>*.

The resultant differences for the Pt/LTL samples are denoted as Δ*μ<sub>ads</sub>*(RED) = *μ<sub>L3</sub>*(RED) − *μ<sub>L3</sub>*(He573), with *μ<sub>L3</sub>*(RED) the Pt L<sub>3</sub> edge after reduction in H<sub>2</sub> at 573 K and *μ<sub>L3</sub>*(He573) the Pt L<sub>3</sub> edge after subsequent treatment in a helium flow for 1 h at 573 K to remove part of the chemisorbed hydrogen.

After evacuation of the Al<sub>2</sub>O<sub>3</sub> samples at 473 K at a pressure of less than 10<sup>−3</sup> Pa, almost all H is removed from the Pt particles. The L<sub>3</sub> XAFS spectrum obtained after evacuation at 473 K is further called the reference spectrum *μ<sub>L3</sub>*(VAC473). The Δ*μ<sub>ads</sub>* obtained after reduction is called Δ*μ<sub>ads</sub>*(RED) = *μ<sub>L3</sub>*(RED) − *μ<sub>L3</sub>*(VAC473). To obtain the (average) signature of the H atoms that remained adsorbed (denoted "ads") on the surface after evacuation at a certain temperature *T*, the reference spectrum *μ<sub>L3</sub>*(VAC473) was subtracted from the corresponding spectrum: Δ*μ<sub>ads</sub>*(*T*) = *μ<sub>L3</sub>*(VAC at *T*) − *μ<sub>L3</sub>*(VAC473) with *T* = 323, 373 and 423 K, respectively. The signature of the incremental (denoted "inc") changes induced by desorption and rearrangement of the remaining H after an evacuation procedure at a certain temperature *T* is reflected by subtracting the spectra of two consecutive evacuation treatments: Δ*μ<sub>inc</sub>*(*T*) = *μ<sub>L3</sub>*(VAC[*T* − 50]) − *μ<sub>L3</sub>*(VAC at *T*).

## Theoretical Methods

Two quite different, but complementary, theoretical calculations are performed on model clusters to interpret the XANES data and understand the results. Density functional calculations (DFT) are utilized to calculate adsorbate–Pt bond energies and optimal adsorbate binding sites. Slater type orbitals are used to represent the atomic orbitals, with basis sets consisting of triple- $\zeta$  quality, extended with two polarization functions. As such these calculations represent the bonding orbitals well, and give good estimates of the bond energies and optimal binding sites. To obtain reliable binding energies, a geometry optimization has to be carried out. However, these calculations do not adequately approximate the antibonding and continuum orbitals 10–50 above the Fermi level, necessary to interpret the XANES data. Therefore, real-space full multiple scattering calculations utilizing a muffin-tin potential are also performed. These calculations effectively approximate the continuum orbitals, and because of the full multiple scattering, also reasonably approximate the strong antibonding resonances present in this energy region. However the latter calculations do not allow accurate estimates of the bond energies or binding sites. The FEFF8 code does not by itself allow geometry optimization, since the total energy is not

(13) Vaarkamp, M.; Mojet, B. L.; Modica, F. S.; Miller, J. T.; Koningsberger, D. C. *J. Phys. Chem.* **1995**, *99*, 16067–16075.

(14) Koningsberger, D. C.; Mojet, B. L.; van Dorssen, G. E.; Koningsberger, D. C. *Top. Catal.* **2000**, *10*, 143–155.

(15) Vaarkamp, M.; Miller, J. T.; Modica, F. S.; Koningsberger, D. C. *J. Catal.* **1996**, *163*, 294–305.

(16) Vaarkamp, M.; Modica, F. S.; Miller, J. T.; Koningsberger, D. C. *J. Catal.* **1993**, *144*, 611–626.

(17) Ramaker, D. E.; Mojet, B. L.; Garriga Oostenbrink, M. T.; Miller, J. T.; Koningsberger, D. C. *Phys. Chem. Chem. Phys.* **1999**, *1*, 2293–2302.



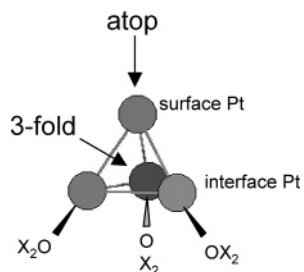


**Figure 3.** Supported Pt<sub>4</sub> model cluster with X<sub>2</sub>O (X = F, H, or Na) molecules mimicking the support.

calculated. However, as will be shown below, the FEFF8 code gives a reliable  $\Delta\mu$  signature of the Pt–H binding site. This signature is not critically sensitive to the Pt cluster geometry, although it is sensitive to the Pt–H bond length.

**Calculations of Pt L<sub>3</sub> XANES Using the FEFF8 Code.** Since the absorption  $\mu$  equals  $\mu_0(1 + \chi)$ , the total change in the L<sub>3</sub> edge due to chemisorption of hydrogen,  $\Delta\mu_{L3} = \mu_{L3}(H/Pt) - \mu_{L3}(Pt)$ , can be expressed as

$$\Delta\mu_{L3} = \mu_{L3}(H/Pt) - \mu_{L3}(Pt) = \Delta\mu_o + \Delta(\mu_o\chi_{Pt-Pt}) + \mu_{o,H/Pt}\chi_{Pt-H} \quad (1)$$

with

$\Delta\mu_{L3}$ : the L<sub>3</sub> edge difference spectrum

$\mu_{L3}(H/Pt)$ : the L<sub>3</sub> edge spectrum in the presence of H<sub>2</sub>

$\mu_{L3}(Pt)$ : the L<sub>3</sub> edge spectrum in a vacuum

$\Delta\mu_o$ : changes in the atomic L<sub>3</sub> XAFS with H coverage

$\Delta(\mu_o\chi_{Pt-Pt})$ : changes in the Pt–Pt total scattering induced by H<sub>2</sub> chemisorption,

$\mu_{o,H/Pt}$ : the free atom L<sub>3</sub> absorption (including atomic XAFS) in the presence of H<sub>2</sub>

$\chi_{Pt-H}$ : the additional Pt–H scattering.

To investigate both the effect of the hydrogen adsorption site (atop vs 3-fold) and the ionicity of the support on the XANES,  $\Delta\mu_{L3}$  spectra were calculated using the FEFF8 code. The FEFF8 code performs *ab initio* self-consistent field, real-space, full multiple scattering calculations. FEFF8 implements self-consistent field potentials for the determination of the Fermi-level and the charge transfer. The calculations were performed using the Hedin–Lundquist exchange correlation potential. A core-hole is included on the absorber atom in order to mimic the final state of the photon absorption process. The calculations were carried out on a supported tetragonal Pt<sub>4</sub> cluster, which is schematically given in Figure 3. To mimic the support, three X<sub>2</sub>O molecules were placed underneath the Pt<sub>4</sub> cluster in a triangular arrangement. For the FEFF8 calculations the ‘support’ X<sub>2</sub>O molecules were taken as H<sub>2</sub>O. Here the O atoms represent the O atoms of the support (either LTL zeolite or alumina) and the H atoms ‘terminate’ the cluster and represent bonds to either the Si or Al atoms of the support. The H<sub>2</sub>O molecules were placed in a flat position beneath the interface Pt. The ionicity of the support was mimicked by changing the electron richness of the oxygen atoms:  $-0.01$  e (ionic) and  $+0.05$  (covalent).<sup>9</sup>

The average Pt–Pt and Pt–O coordination numbers for these Pt<sub>4</sub>/X<sub>6</sub>O<sub>3</sub> clusters are 3 and 0.75, respectively. The Pt clusters in the LTL support are very small and have average Pt–Pt coordination numbers of around 4. The Pt–O coordination number in the model cluster is somewhat bigger than that seen in the experimental data (typically 0.2–0.5). In the FEFF8 calculations (no geometry optimization), the atop site hydrogen adsorption was mimicked by placing three hydrogen on top of the surface Pt atom (atop site is pictured in Figure 3), giving an average Pt–H coordination number of 0.75. Three-fold site hydrogen adsorption was realized by placing hydrogen in each of the 3-fold sites

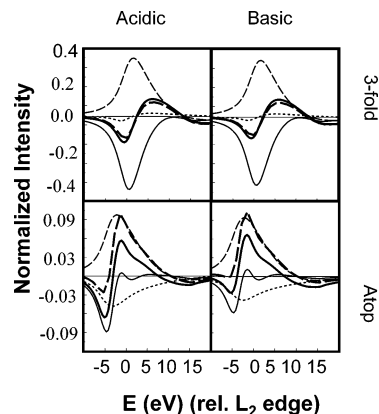


**Figure 4.** Schematic representation of the signature of  $\Delta\mu_{L3} = \mu_{L3}(Pt-H) - \mu_{L3}(Pt)$  and its contributions as a function of adsorption site. Thick solid line:  $\Delta\mu_{L3}$  (total) including all contributions, thick dashed line:  $\Delta\mu_{L3}$  (total) minus  $\Delta\mu_o$  (change in AXAFS), thin dashed line:  $\mu_o\chi_{Pt-Pt}$  (Pt–H scattering), thin solid line:  $\mu_o\chi_{Pt-Pt}$  (change in Pt–Pt scattering), and dotted line:  $\Delta\mu_o$  (change in AXAFS).

(see Figure 3), leading to an average Pt–H coordination number of 2.25. In both cases, the Pt–H distance was fixed at 1.9 Å. The oxygen atoms are placed at 2.2 Å from the Pt atoms in the Pt<sub>4</sub> cluster, distances typically found in the EXAFS data. Two different types of Pt atoms can be distinguished in the supported Pt<sub>4</sub> cluster: Pt<sub>surf</sub> and Pt<sub>int</sub>. The theoretical X-ray spectrum of the supported cluster ( $\mu$ ) was obtained by calculating  $\mu(Pt_{surf})$  and  $\mu(Pt_{int})$  followed by averaging:  $\mu = 1/4 \mu(Pt_{surf}) + 3/4 \mu(Pt_{int})$ , as would be reflected in an experimental spectrum.

The results of the calculations are given in Figure 4. Since the H adsorbed in the bridged and 3-fold position yield essentially the same calculated spectral line shapes for  $\Delta\mu_{L3}$ , these sites are further referred to as the *n*-fold site with *n*=2 or 3, respectively. Figure 4 shows that when the H is placed in the *n*-fold position, the change in the Pt–Pt scattering (the  $\mu_o\chi_{Pt-Pt}$  term, the thin solid line) is the largest. This originates from a destabilization of the Pt–Pt bonds beneath the H. Thus the Pt–Pt multiple scattering is strongly reduced in the presence of the H, and this appears as a large negative contribution in the  $\mu_o\chi_{Pt-Pt}$  term. The effect of the  $\mu_o\chi_{Pt-H}$  term (thin dashed line) is somewhat smaller in size and positive. The difference in the atomic XAFS (AXAFS) contribution (dotted line) is small. The total of all terms ( $\Delta\mu_{L3}$ ) is indicated in Figure 4 with a thick solid line. For the *n*-fold site not much difference can be observed between the covalent and ionic supports. Moreover, the change in the atomic XAFS ( $\Delta\mu_o$ ) has hardly any effect on the total  $\Delta\mu_{L3}$ , which can be seen by comparing the thick solid line (total  $\Delta\mu_{L3}$ ) with the thick dashed line,  $\Delta\mu_{L3} - \Delta\mu_o$ .

When H is adsorbed in the atop position, the theoretically obtained  $\Delta\mu_{L3}$  has to be shifted to lower energy in order to fit the experimental data for Pt particles on covalent supports (see Supporting Information). The hydrogen induced change in the Pt–Pt scattering ( $\mu_o\chi_{Pt-Pt}$ ; thin solid line) is about 10 times smaller in amplitude and about half in energy width. The Pt–H scattering (the  $\mu_o\chi_{Pt-H}$  term, the thin dashed line in Figure 4) is nearly independent of the H binding site, only its amplitude is about 4 times smaller. The AXAFS  $\Delta\mu_o$  term (dotted line in Figure 4) appears to be much more negative upon moving the H from the 3-fold to the atop position. Calculations suggest that this may result from a change in the direction of the charge transfer, but the magnitude of this charge transfer is very small for all adsorption sites. Now the change in the atomic XAFS ( $\Delta\mu_o$ ) has an effect on the total  $\Delta\mu_{L3}$ , which can be seen by comparing the thick solid line (total  $\Delta\mu_{L3}$ ) with the thick dashed line ( $\Delta\mu_{L3} - \Delta\mu_o$ ). Also for the atop site not much difference can be observed between the ionic and covalent supports.

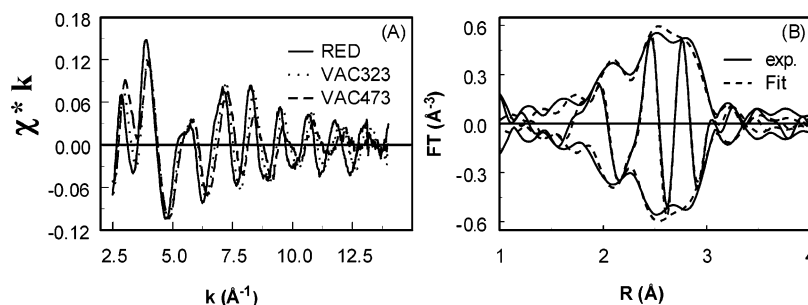


**Figure 5.** (A)  $k^1$  weighted raw EXAFS spectra of Pt/K–Al<sub>2</sub>O<sub>3</sub> after reduction at 673 K (solid line), after evacuation at 323 K (dotted line) and after evacuation at 473 K (dashed line). (B) Fourier transform ( $k^2$ ,  $2.5 < k < 14 \text{ \AA}^{-1}$ ) of the spectrum taken after reduction at 673 K (solid line) and best  $R$ -space fit ( $1.6 < R < 3.2 \text{ \AA}$ , dashed line).

In earlier work<sup>6,17,18,19,20</sup> we attributed the changes in the Pt L<sub>3</sub> X-ray absorption near edge data induced by chemisorption of hydrogen entirely to the formation of a chemical bond between Pt and hydrogen (i.e., only to the 3rd term in eq 1). The availability of the FEFF8 code made it possible to reinvestigate the changes in the Pt near edge X-ray absorption data.<sup>2,3</sup> This reinvestigation revealed that significant changes also occur in the Pt–Pt scattering upon adsorption of hydrogen, and this change, as shown above, is highly dependent on the H adsorption site. Thus the XANES  $\Delta\mu$  technique can now be used to monitor the type of hydrogen adsorption site on the surface of the Pt particles (see further in Supporting Information).

**Density Functional Calculations (DFT).** The Amsterdam Density Functional Package (ADF)<sup>21</sup> was used to perform DFT calculations on the supported Pt<sub>4</sub> model cluster as given in Figure 3. Relativistic effects were accounted for in the calculations. To enhance computational efficiency, several atomic core shells of the Pt atoms were frozen up to and including the Pt 4d level. The geometry optimizations were carried out in the spin-unrestricted mode (the spin state is taken into account) at the GGA (generalized gradient approximation) level including scalar relativistic effects. Olsen et al.<sup>22</sup> showed that this level of accuracy provides good agreement with experiments for the interaction of H and platinum. The numerical integration precision applied was set to 5.5 significant digits. The applied criteria for the geometry optimization were  $1 \times 10^{-3}$  Hartrees for the changes in energy,  $1 \times 10^{-4}$  Hartree/Å for changes in the energy gradients, and  $1 \times 10^{-2}$  Å for changes in the Cartesian coordinates.

By changing the nature of the X atoms from Na to F, a change in ionicity of the support can be simulated. Since F is more electronegative than Na, the oxygen atoms are electron rich in the presence of Na and electron poor in the presence of F, thereby simulating a change in electron richness on the support oxygen atoms going from acidic (X = F) to basic (X = Na) supports. It should be noted here that the utilization of 6 Na and 6 F atoms so close to a Pt<sub>4</sub> cluster probably represents the extreme of ionic (basic) to covalent or acidic supports.

In these calculations, a single H atom was placed near the supported Pt<sub>4</sub> clusters. The Pt<sub>4</sub> cluster and H atom were allowed to relax their geometry within the restrictions of C(S) symmetry and with the X<sub>2</sub>O molecules kept at fixed positions. The cluster and adsorbate positions are depicted in Figure 3. These calculations were repeated with 2 H atoms now allowing both H atoms to move to optimal bonding sites as dictated by minimum energy (i.e., the geometries of these clusters were fully optimized in the ADF calculations to obtain reasonable estimates of the Pt-adsorbate bond energies). The results reflect the Pt–H and

**Table 1.** EXAFS Fit Results for Sample Pt/K–Al<sub>2</sub>O<sub>3</sub><sup>a</sup>

| treatment | scatterer | N<br>(±10%) | R (Å)<br>(±0.02 Å) | $\Delta\sigma^2$<br>( $\times 10^3$ , ±5%) | $E_0$ (eV)<br>(±10%) | variance % |        |
|-----------|-----------|-------------|--------------------|--|----------------------|------------|--------|
|           |           |             |                    |  |                      | FT im      | FT abs |
| RED       | Pt        | 6.5         | 2.75               | 4.1  | 1.2                  | 0.868      | 0.308  |
|           | O         | 0.3         | 2.10               | 2.0  | −8.0                 |            |        |
| VAC323    | Pt        | 6.5         | 2.71               | 5.6  | −0.3                 | 0.414      | 0.135  |
|           | O         | 0.3         | 2.10               | 4.0  | −7.3                 |            |        |
| VAC373    | Pt        | 6.5         | 2.71               | 5.0  | −0.2                 | 0.700      | 0.321  |
|           | O         | 0.4         | 2.10               | 4.0  | −7.0                 |            |        |
| VAC423    | Pt        | 5.7         | 2.69               | 5.0  | 0.1                  | 1.59       | 0.993  |
|           | O         | 0.5         | 2.10               | 4.0  | −7.0                 |            |        |
| VAC473    | Pt        | 5.4         | 2.68               | 6.6  | −0.6                 | 2.07       | 0.632  |
|           | O         | 0.7         | 2.10               | 4.0  | −2.6                 |            |        |

<sup>a</sup> Fits were done in  $R$ -space,  $k^2$  weighting,  $1.6 < R < 3.2 \text{ \AA}$  and  $\Delta k = 2.5\text{--}14 \text{ \AA}^{-1}$ . The Debye Waller factors ( $\Delta\sigma^2$ ) were multiplied by  $10^3$  and are relative to the references. Accuracy limits are given between brackets

Pt–O<sub>support</sub> bond lengths typical of that found from the EXAFS results and other reported theoretical results<sup>5,23,24,25</sup> (to be discussed below).

## Results

**EXAFS Data Analysis.** In Figure 5A, the raw EXAFS data for the Pt/K–Al<sub>2</sub>O<sub>3</sub> catalyst after reduction at 673 K, evacuation at 323 and 473 K are shown. The quality of the data is representative for all spectra. The evacuation treatment clearly changes the nodes of the oscillations. The distance between the nodes is smallest after reduction at 673 K and increases when the catalyst is evacuated at a higher temperature. This indicates a decrease in the Pt–Pt bond length when the Pt/K–Al<sub>2</sub>O<sub>3</sub> catalyst is evacuated at higher temperatures. After evacuation the amplitude of the EXAFS oscillations decays faster with increasing values of  $k$ , pointing to an increase in disorder due to the removal of hydrogen.

The Fourier Transform ( $k^2$  weighted,  $2.5 < k < 14 \text{ \AA}^{-1}$ ) of the EXAFS data for the reduced Pt/K–Al<sub>2</sub>O<sub>3</sub> catalysts is shown in Figure 5B (solid line). Data analysis has been performed by multiple shell fitting in  $R$  space ( $1.6 < R < 3.2 \text{ \AA}$ ). By using the difference file technique<sup>26</sup> a Pt–Pt and a Pt–O contribution could be visually identified. The variances of the fits of the imaginary and absolute part of the Fourier transform were used to determine the fit quality. The fit is shown in Figure 5B (dotted line). The quality of fit is representative for all data. The

- (18) Koningsberger, D. C.; de Graaf, J.; Mojet, B. L.; Ramaker, D. E.; Miller, J. T. *Appl. Catal. A* **2000**, *191*, 205–220.
- (19) Mojet, B. L.; Ramaker, D. E.; Miller, J. T.; Koningsberger, D. C. *Catal. Lett.* **1999**, *62*, 15–20.
- (20) Koningsberger, D. C.; Oudenhuijzen, M. K.; Bitter, J. H.; Ramaker, D. E. *Top. Catal.* **2000**, *10*, 167–177.
- (21) Amsterdam Density Functional Package ADF 2000.02, Department of Theoretical Chemistry, Vrije Universiteit, Amsterdam. <http://www.scm.com>.
- (22) Olsen, R. A.; Kroes, G. J.; Baerends, E. J. *J. Chem. Phys.* **1999**, *111*, 11155–11163.

- (23) Papoian, G.; Nørskov, J. K.; Hoffmann, R. *J. Am. Chem. Soc.* **2000**, *122*, 4129–4144.
- (24) Feibelman, P. J.; Hamann, D. R. *Surf. Sci.* **1987**, *182*, 411–422.
- (25) Davis, S. M.; Somorjai, G. A. *The Chemical Physics of Solid Surfaces and Heterogeneous Catalysts*; King, D. A., Woodruff, D. P. Eds.; Elsevier Publishers Amsterdam, **1982**, *4*, 271.
- (26) Koningsberger, D. C.; Mojet, B. L.; van Dorssen, G. E.; Ramaker, D. E. *Topics Catal.* **2000**, *10*, 143–155.

**Table 2.** EXAFS Fit Results for Sample Pt/Cl–Al<sub>2</sub>O<sub>3</sub><sup>a</sup>

| treatment | scatterer | N                 | R (Å)           | $\Delta\sigma^2$           | $E_0$ (eV)     | variance % |        |
|-----------|-----------|-------------------|-----------------|----------------------------|----------------|------------|--------|
|           |           | ( $\pm 10\%$ )    | ( $\pm 0.02$ Å) | ( $\times 10^3, \pm 5\%$ ) | ( $\pm 10\%$ ) | FT im      | FT abs |
| RED       | Pt        | 8.8               | 2.76            | 2.5                        | −0.2           | 0.527      | 0.319  |
|           | O         | n.d. <sup>b</sup> |                 |                            |                |            |        |
| VAC323    | Pt        | 7.9               | 2.74            | 3.6                        | −0.5           | 0.459      | 0.126  |
|           | O         | 0.2               | 2.05            | 5.0                        | 0.0            |            |        |
| VAC373    | Pt        | 7.3               | 2.73            | 2.6                        | −0.2           | 0.666      | 0.177  |
|           | O         | 0.3               | 2.09            | 4.0                        | −5.0           |            |        |
| VAC423    | Pt        | 7.8               | 2.73            | 3.3                        | −0.2           | 0.466      | 0.139  |
|           | O         | 0.3               | 2.07            | 4.0                        | 5.0            |            |        |
| VAC473    | Pt        | 7.7               | 2.73            | 3.4                        | −0.4           | 0.951      | 0.429  |
|           | O         | 0.4               | 2.07            | 5.0                        | 5.0            |            |        |

<sup>a</sup> Fits were done in *R*-space,  $k^2$  weighting,  $1.6 < R < 3.2$  Å and  $\Delta k = 2.5$ – $14$  Å<sup>−1</sup>. The Debye Waller factors ( $\Delta\sigma^2$ ) were multiplied by  $10^3$  and are relative to the references. Accuracy limits are given between brackets.

<sup>b</sup> This contribution was too small to be fitted.

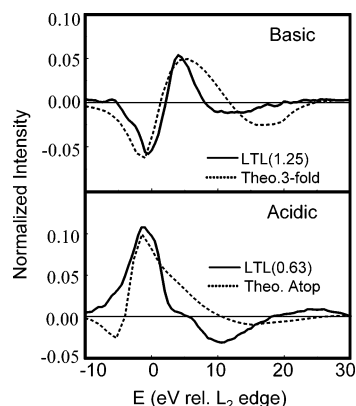


**Figure 6.** Comparison of the experimental difference spectra,  $\Delta\mu_{\text{ads}} = \mu_{\text{L3}}(\text{H}/\text{Pt}) - \mu_{\text{L3}}(\text{Pt})$ , (solid lines) for LTL(*x.x*) (*x.x* indicating K/Al ratio data), with the optimally aligned theoretical FEFF8 fingerprints (dotted lines) obtained from Figure 4. It should be noted here that the dotted lines represent the theoretical  $\Delta\mu_{\text{L3}} - \Delta\mu_0$  curves (see appendix).

resulting EXAFS coordination parameters are given in Table 1 (Pt/K–Al<sub>2</sub>O<sub>3</sub> catalyst) and Table 2 (Pt/Cl–Al<sub>2</sub>O<sub>3</sub>).

The Pt particle size after reduction in the Pt/K–Al<sub>2</sub>O<sub>3</sub> catalyst is smaller than in the Pt/Cl–Al<sub>2</sub>O<sub>3</sub> catalyst (coordination number,  $N_{\text{Pt-Pt}} = 6.5$  vs 8.8). Further, the Pt/K–Al<sub>2</sub>O<sub>3</sub> sample shows a larger decrease of the Pt–Pt coordination distance after evacuation at 473 K (Pt/K–Al<sub>2</sub>O<sub>3</sub>:  $\Delta R = 0.08$  Å; Pt/Cl–Al<sub>2</sub>O<sub>3</sub>:  $\Delta R = 0.03$  Å). For both catalysts, the evacuation treatment leads to a small decrease of the Pt–Pt coordination number (with a smaller decrease for the larger Pt particles on Pt/Cl–Al<sub>2</sub>O<sub>3</sub>) and an increase in the Pt–O coordination number.

**Near Edge Analysis of the Pt L<sub>3</sub> X-ray Absorption Edges.** The  $\Delta\mu_{\text{ads}}$  (RED) =  $\mu_{\text{L3}}(\text{RED}) - \mu_{\text{L3}}(\text{He573})$  signatures for Pt/LTL(1.25) and Pt/LTL(0.63) are given in Figure 6 with a solid line. The theoretical signatures ( $\Delta\mu_{\text{L3}} - \Delta\mu_0$ ) are indicated with a dotted line. By comparing the theoretical with the experimental signatures one can conclude that under the given experimental conditions the hydrogen is chemisorbed in a 3-fold Pt site for the basic and in an atop Pt site for the acidic Pt/LTL catalysts. The theoretical signature ( $\Delta\mu_{\text{L3}} - \Delta\mu_0$ ) mimics the experimental data the best. The rationale for the use of  $\Delta\mu_{\text{L3}} - \Delta\mu_0$  as theoretical signature instead of  $\Delta\mu_{\text{L3}}$  is extensively discussed in the Supporting Information.

For the much larger Pt particles supported on Al<sub>2</sub>O<sub>3</sub>, the L<sub>3</sub> X-ray absorption edges obtained after the various experiments

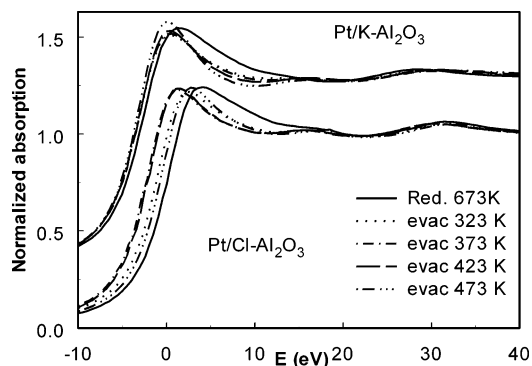


**Figure 7.** L<sub>3</sub> edges (after the alignment procedure) for both Pt/Cl–Al<sub>2</sub>O<sub>3</sub> and Pt/K–Al<sub>2</sub>O<sub>3</sub> catalysts after the various pretreatments.

on the Al<sub>2</sub>O<sub>3</sub> samples are shown in Figure 7. Clearly, the edge position and whiteline intensity are influenced by the amount of H adsorbed on the sample. The  $\Delta\mu_{\text{inc}}(T)$  and  $\Delta\mu_{\text{ads}}(T)$  difference spectra are displayed in Figure 8 (A,B: Pt/Cl–Al<sub>2</sub>O<sub>3</sub> and C,D: Pt/K–Al<sub>2</sub>O<sub>3</sub>). These data show more detailed changes than for the much smaller Pt particles dispersed in the LTL zeolites (compare with Figure 6).  $\Delta\mu_{\text{ads}}(T)$  reflects the H that remains on the surface after an evacuation step,  $\Delta\mu_{\text{inc}}(T)$  reflects the effect of H desorption and a possible rearrangement of the remaining H as a result of the temperature change. Therefore, the solid lines in Figure 8B,D should reflect the total amount of hydrogen present at RT after reduction on the surface of the Pt particles dispersed on Cl–Al<sub>2</sub>O<sub>3</sub> and K–Al<sub>2</sub>O<sub>3</sub>, respectively. However, it can be seen that the amplitudes of the solid lines are much smaller than the lines representing the amount of hydrogen present on the Pt surface after further evacuation at higher temperature. This can be explained by noting that the atop and *n*-fold  $\Delta\mu$  signatures are partially in “antiphase” of each other. Assuming that after reduction in hydrogen, H is chemisorbed both in atop and 3-fold sites (i.e., ontop and 3-fold H), the overall signature will show a strong interference between the two individual signatures that are in antiphase. This leads to a small amplitude in the resulting curve as observed in Figure 8B,D. Further evacuation at higher temperatures will then finally lead to the signature of the type of hydrogen site that remains occupied after the specific evacuation treatment. It can be seen that after evacuation at 373 K ( $\Delta\mu_{\text{ads}}(373) = \mu_{\text{L3}}(\text{VAC373}) - \mu_{\text{L3}}(473)$ , dashed dotted lines) hydrogen is chemisorbed in an atop Pt site for the Pt/Cl–Al<sub>2</sub>O<sub>3</sub> and stays chemisorbed in a 3-fold Pt site for the Pt/K–Al<sub>2</sub>O<sub>3</sub> catalysts. The same situation is still present after evacuation at 423 K (dashed lines). At the same time, Figure 8A,C ( $\Delta\mu_{\text{inc}}(423) = \mu_{\text{L3}}(\text{VAC 373}) - \mu_{\text{L3}}(\text{VAC 423})$ , dotted dashed lines) show that evacuation at 423 K leads to the disappearance of chemisorbed hydrogen from an atop Pt site on the Pt/Cl–Al<sub>2</sub>O<sub>3</sub> and from a 3-fold Pt site on the Pt/K–Al<sub>2</sub>O<sub>3</sub> sample.

**DFT Calculations.** The calculated binding energies of one and two H atoms on the different supported Pt<sub>4</sub> clusters are given in Table 3. The binding energy  $E_b$  is calculated as the difference between molecular H<sub>2</sub> and a clean, supported Pt<sub>4</sub> cluster, in kJ/mol H<sub>2</sub> and with *n* H atoms on the Pt<sub>4</sub> cluster

$$E_b = \frac{2}{n}E_{\text{Pt}_4+n\text{H}} - \frac{2}{n}E_{\text{Pt}_4} - E_{\text{H}_2} \quad (2)$$

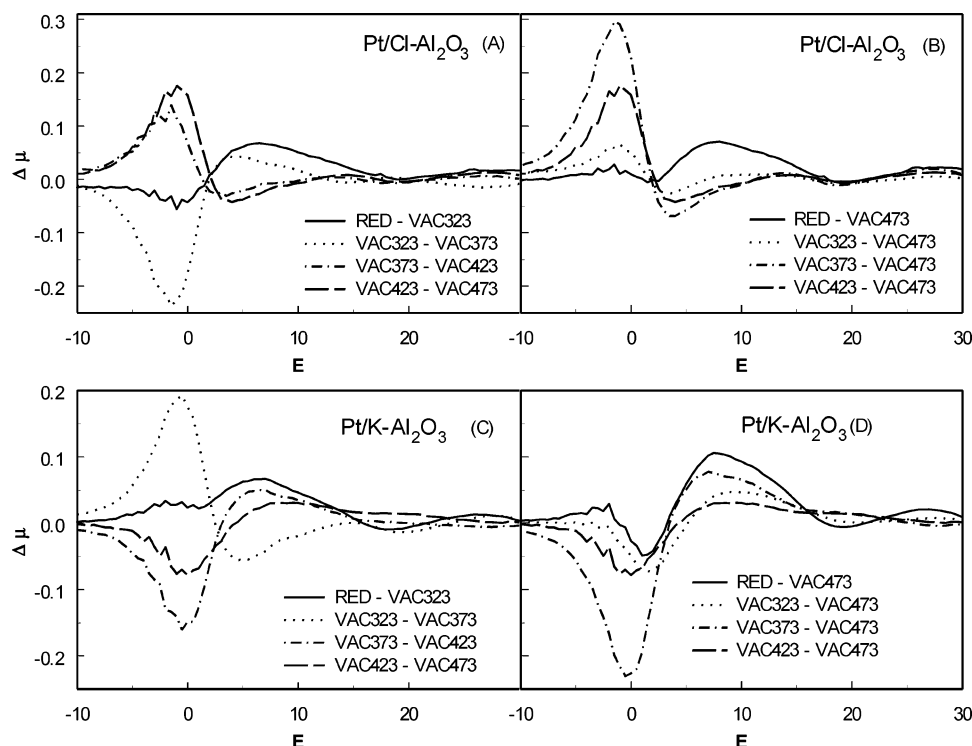


**Figure 8.** Difference spectra of the XANES region for the  $L_3$  edges for Pt/Cl- $\text{Al}_2\text{O}_3$ : (A)  $\Delta\mu_{\text{inc}}(T)$  and (B)  $\Delta\mu_{\text{ads}}(T)$ , and Pt/K- $\text{Al}_2\text{O}_3$ : (C)  $\Delta\mu_{\text{inc}}(T)$  and (D)  $\Delta\mu_{\text{ads}}(T)$ .

**Table 3.** Binding Energies (kJ/mol) with Respect to Gas Phase  $\text{H}_2$  and Equilibrium Distances (Å) of H as a Function of Coverage, Position and Support Ionicity

| no. of<br>H atoms | Pt <sub>4</sub> /F <sub>2</sub> O |  | Pt <sub>4</sub> /Na <sub>2</sub> O |  | position <sup>a</sup> | spin |
|-------------------|-----------------------------------|--|------------------------------------|--|-----------------------|------|
|                   | $E_b$<br>(kJ/mol $\text{H}_2$ )   | $R_{\text{Pt-H}}$ (Å)                  | $E_b$<br>(kJ/mol $\text{H}_2$ )    | $R_{\text{Pt-H}}$ (Å)                  |                       |      |
| 1 H               | -77                               | 1.55                                   | -150                               | 1.59                                   | atop                  | 1/2  |
| 2 H               | -71                               | 1.68 <sup>b</sup><br>1.77 <sup>c</sup> | -77                                | 1.74 <sup>b</sup><br>1.70 <sup>c</sup> | bridged               | 0    |

<sup>a</sup> This was the optimal position. When H was placed in another position, the H drifted away. <sup>b</sup> Distance from the surface Pt atom to the H. <sup>c</sup> Distance from the interface Pt atom to the H.

The required atomic reference energies are obtained according to Baerends et al.<sup>27</sup> When only 1 H atom is chemisorbed on the Pt<sub>4</sub> cluster, the most stable position is the atop site. A single H atom in a 3-fold site is unstable with respect to the atop site, so that in the geometry optimization, the H atom simply moves to the atop site, exactly as was found by Kua and Goddard.<sup>5</sup> The calculated binding energy is clearly also dependent on the ionicity properties of the support. The Pt-H binding energy for the ionic support Pt/Na<sub>2</sub>O is -150 kJ/mol, which is 73 kJ/mol stronger than for the more covalent support (Pt/F<sub>2</sub>O: -76.6 kJ/mol). This large difference arises in part because of the extreme difference in ionicity of our small model Pt<sub>4</sub>/(A<sub>2</sub>O)<sub>3</sub> cluster; however, the increased value for the basic support is correct. When the H coverage is increased to 2 H atoms on the Pt<sub>4</sub> cluster, the 2-fold sites (bridged) turned out to be the most favored for H chemisorption. No hydrogen is chemisorbed any longer in an atop site. The Pt-H binding energy for the Pt/Na<sub>2</sub>O is still higher by 6 kJ/mol in comparison to Pt/F<sub>2</sub>O. The

Pt-H bond distance depends on the adsorption site: 1.55–1.60 Å in the case of the atop site, and 1.68–1.77 Å in the 2-fold. The optimal doublet state is the optimal spin state for the supported Pt<sub>4</sub> clusters with 1 H atom, the singlet state is optimal for 2 adsorbed H atoms.

## Discussion

**Effect of Metal Particle Size and H Coverage on the EXAFS Region.** As already mentioned, the EXAFS data-analysis and the resulting EXAFS coordination parameters of the Pt/LTL samples were given and discussed in an earlier paper.<sup>8</sup> The Pt-Pt coordination number was found to be around 4 and points to extremely small Pt particles consisting of 5–6 atoms with similar size in the acidic (0.63), neutral (0.96) and basic (1.25) LTL. The Pt-Pt distance decreased by about 0.03 Å after the treatment in He. The contraction of the first shell Pt-Pt coordination upon removal of chemisorbed hydrogen is due to the cancellation of the hydrogen induced Pt-Pt bond weakening, called d-electron frustration by Feibelman,<sup>24</sup> and Pt-Pt destabilization by Papoian et al.<sup>23</sup> Therefore, the contraction of the first shell distance clearly reveals that the He treatment removes (some) hydrogen from the Pt surface.

The average size of the Pt particles on Al<sub>2</sub>O<sub>3</sub> are much larger than those in the LTL zeolite, but those in K-Al<sub>2</sub>O<sub>3</sub> are smaller than those in Pt/Cl-Al<sub>2</sub>O<sub>3</sub>. Consequently, the influence of H removal on the contraction of the Pt-Pt distance is largest for the Pt particles on the K-Al<sub>2</sub>O<sub>3</sub> support. The Pt-Pt bond length decreases from 2.75 Å after reduction to 2.71 Å after evacuation at 323 K. It decreases even further to 2.68 Å after evacuation at 473 K, leading to a total decrease of 0.07 Å. Despite the fact that the Pt particles supported on Al<sub>2</sub>O<sub>3</sub> are larger than the Pt particles dispersed in the LTL zeolite, the decrease in Pt-Pt distance is much larger. This is due to the more severe

(27) Baerends E. J.; Branchadell V.; Sodupe M. *Chem. Phys. Lett.* **1997**, 265, 481–489.



evacuation treatment applied on the  $\text{Al}_2\text{O}_3$  supported Pt particles, leading to the removal of a higher fraction of chemisorbed hydrogen.

The small but noticeable decrease in Pt–Pt coordination after hydrogen removal can be explained by a slight flattening out of the Pt particles onto the  $\text{Al}_2\text{O}_3$  support in order to minimize the effect of the coordinative unsaturation of the surface Pt atoms. The increase in disorder of the Pt–Pt coordination can also be explained by this small change in morphology. The reduction of the Pt–Pt bond length<sup>28</sup> and flattening of the particle induced by H desorption are well-known phenomena for supported metal particles.<sup>6</sup> In addition, the Pt–O coordination number increases from 0.3 to 0.8 with increasing temperature of evacuation. The increase in Pt–O coordination can be explained by an increase in the metal–support interface area after removal of chemisorbed H. The EXAFS results for Pt/Cl– $\text{Al}_2\text{O}_3$  show similar trends, but due to the larger size of the Pt particles the effects due to the desorption of H are smaller.

**DFT Calculations.** The DFT calculations, as summarized in Table 3, show that regardless of the ionicity of the support, the first H atom preferentially adsorbs on the atop site. This preference for the atop site on Pt was also suggested by the results of Olsen et al.<sup>22</sup> and Kua and Goddard.<sup>5</sup> Further, in the case of an ionic support ( $\text{Pt}_4/\text{Na}_2\text{O}$ ), the Pt–H bond energy is much larger ( $-150$  kJ/mol) than for a covalent support ( $\text{Pt}_4/\text{F}_2\text{O}$ ) ( $-77$  kJ/mol). To compare these bond strength values with literature data one can assume that a neutral support does not influence the electronic structure of Pt. Therefore, the average bond energy of about  $-110$  kJ/mol can be compared with  $\Delta H$  values of  $-35 \pm 20$  kJ/mol  $\text{H}_2$ <sup>29</sup> as found from literature data for Pt–H bonded on a Pt(111) surface. The large difference can be fully attributed to the highly unsaturated Pt atoms in the case of the  $\text{Pt}_4$  cluster under study (all corner atoms). However, the observed small Pt–H bond length of  $1.55$ – $1.60$  Å for the atop position<sup>23</sup> is in good agreement with other theoretical results reported in the literature.

Regardless of the ionicity of the support, at higher coverage (2 H atoms on a  $\text{Pt}_4$  cluster), the DFT results indicate the H atoms preferentially adsorb in the  $n$ -fold (bridge) positions. The calculations show that no hydrogen is chemisorbed any longer in an atop site. This can be explained by the strong lateral interaction between the two hydrogen atoms, leading to an  $n$ -fold type of adsorption. The Pt–H binding energy is much lower than for the atop Pt site. However, the Pt–H binding energy for  $\text{Pt}/\text{Na}_2\text{O}$  is still higher by 6 kJ/mol in comparison to  $\text{Pt}/\text{F}_2\text{O}$ . The large difference between the  $\text{Pt}_{\text{int}}$ –H distance of  $1.77$  Å and  $\text{Pt}_{\text{surf}}$ –H distance of  $1.68$  Å in the case of the covalent  $\text{F}_2\text{O}$  support indicates that H atom in the 2-fold sites are not bonding equally to the 3 Pt atoms. On the basic  $\text{Na}_2\text{O}$  support molecules, the  $\text{Pt}_{\text{surf}}$ –H and  $\text{Pt}_{\text{int}}$ –H are more similar,  $1.70$  and  $1.74$  Å respectively. This indicates that the H adsorption position for Pt on a ionic support ( $\text{Na}_2\text{O}$ ) is much closer to 2-fold symmetry than for Pt on the covalent support ( $\text{F}_2\text{O}$ ); but again we must indicate that the  $\text{Pt}_4/(\text{X}_2\text{O})_3$  model cluster probably exaggerates the affect of the ionicity.

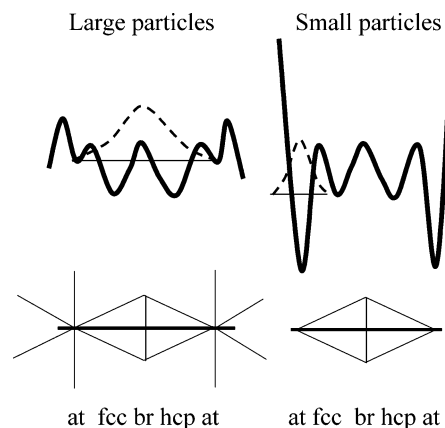


**Figure 9.** Schematic illustration of the difference in potential well for atop sites as a function of the number of Pt neighboring atoms. For large particles hydrogen hops between fcc and hcp sites.

From these DFT calculations, we conclude the following:

- The strongest bonded H is chemisorbed in the atop sites.
- Lateral interactions force this H to move to the  $n$ -fold sites with increasing coverage; thereby allowing the atop sites to be recovered with H as ontop H at higher coverage.
- The H bond strength in the atop sites increases significantly with decreasing Pt–Pt coordination and with increasing electron richness of the support O atoms.
- The binding energies of the different hydrogen adsorption sites therefore increase in the order ontop <  $n$ -fold < atop.

**Transition from Delocalized to Atop H.** The strongest bonded H, existing in atop sites observed on intermediate and small Pt particles can be related to the presence of the most strongly bonded delocalized hydrogen on large Pt particles ( $N > 9$ ) as indicated on the left side in Figure 1. Delocalized hydrogen occurs when the fcc, bridged, and hcp sites have similar binding energy, allowing the H atoms to lower their zero-point vibrational energy by delocalizing over these sites.<sup>30,31,32</sup> This is schematically shown in Figure 9, where the different sites on the surface of large particles (fcc, bridge, hcp) are shown together with the corresponding potential wells. For large Pt particles, the coordination of each Pt is high, leading to a similar potential well depth for the atop site. For small Pt particles this situation is completely different. The corner sites are highly coordinatively unsaturated, leading to a very deep potential well. These corner sites (essentially atop sites) are now favored for hydrogen chemisorption, so that the strongest bonded H, which on polycrystalline Pt is delocalized, now settles into the atop sites.

**Experimental Confirmation for Increasing Atop/On-top Pt–H Binding Energy with Decreasing Particle Size.** Figure 1 (center) has been constructed to be consistent with the Pt/ $\text{Al}_2\text{O}_3$  XANES  $\Delta\mu$  data in Figure 9. Here, the  $\Delta\mu_{\text{inc}}$  data (left side of Figure 9) most directly determines the  $T_{\text{vac}}$  attributed to the different sites in Figure 1(center). Both of the  $\Delta\mu_{\text{inc}}(323) = \mu_{\text{L3}}(\text{Red}) - \mu_{\text{L3}}(\text{VAC } 323)$  curves (Figure 8A,C, solid lines) show that the hydrogen leaving the surface in this temperature increment must have left from both the atop and  $n$ -fold sites, consistent with the small magnitude and double maxima arising

(28) Delley, B.; Ellis, D. E.; Freeman, A. J.; Baerends, E. J.; Post, D. *Phys. Rev. B*, **1983**, *27*, 2132–2144.  
 (29) Ramaker, D. E.; Teliska, M.; Zhang, Y.; Stakheev, A. Yu.; Koningsberger, D. C. *PCCP*, **2003**, *5*, 4492–4501. Average binding energy from Table 2 and Figure 9 shows  $E_b$  to be  $-235 \pm 20$  kJ/mol and assuming  $\Delta H$  for  $\text{H}_2$  is  $-436$  kJ/mol gives  $-35 = -2 \times 235 + 436$ .

(30) Badescu, S. C.; Salo, P.; Ying, S. C.; Jacobi, K.; Wang, Y.; Berdurfing, K.; Ertl, G. *Phys. Rev. Lett.* **2001**, *88* (13), 136101–136104.  
 (31) Kallen, G.; Wahnstrom, G. *Phys. Rev. B*, **2001**, *65* (3), 334061–334063.  
 (32) Nobuhara, K.; Nakanishi, H.; Kasai, H.; Okiji, A. *J. Appl. Phys.* **2000**, *88* (11), 6897–6901.



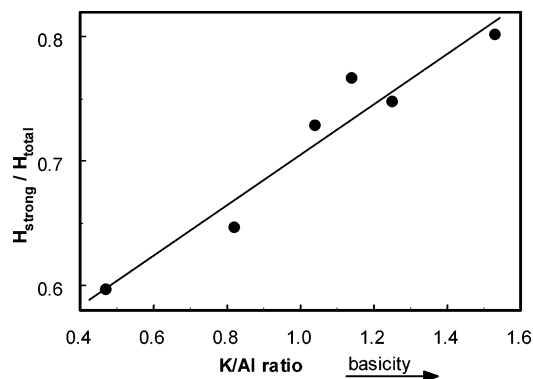


**Figure 10.** Amount of strongly adsorbed H relative to the total amount of H adsorbed as a function of support basicity.

from the interference of the ontop and  $n$ -fold signatures in anti phase as discussed above. However, in the next temperature increment, the  $\Delta\mu_{\text{inc}}(373) = \mu_{\text{L3}}(323) - \mu_{\text{L3}}(373)$  line shape (Figure 8A,C, dotted lines) indicates that  $n$ -fold hydrogen leaves the Pt surface of the Pt/Cl–Al<sub>2</sub>O<sub>3</sub> and atop hydrogen from Pt/K–Al<sub>2</sub>O<sub>3</sub>. This is explained in Figure 1 by the different placement of the ontop sites relative to the  $n$ -fold face sites on the acidic and basic supports. Both of the next two temperature increments, 373–423 and 423–473 show atop and  $n$ -fold signatures for Pt/Cl–Al<sub>2</sub>O<sub>3</sub> (covalent) and Pt/K–Al<sub>2</sub>O<sub>3</sub> (ionic), respectively. Figure 1 explains this behavior by placing the atop and  $n$ -fold edge sites in this temperature range for the covalent (or acid) and ionic (basic) supports, respectively.

Comparison in Figure 1 of the temperatures in a vacuum where the different binding sites desorb for polycrystalline Pt and supported intermediate Pt particles dramatically show the shifts in the ontop and atop sites relative to the  $n$ -fold face and edge sites with decreasing particle size and increasing ionicity of the support. This is fully supported by our discussion of the DFT results and Figure 10. As the particles become smaller and the corner and edges become sharper, the Pt–Pt coordination of the corner atoms becomes smaller, and hence the Pt–H bond energy increases. Further, the DFT calculations show that the atop H bond energy shifts much more than the  $n$ -fold bond energy.

**Determination of Strongly Bonded H Binding Sites on Small Pt Particles.** The very small Pt particles dispersed in LTL zeolite have only corner and edge Pt atoms. As indicated previously<sup>3</sup> and summarized again in Figure 6,  $\Delta\mu_{\text{ads}} = \mu_{\text{L3}}(\text{RED}) - \mu_{\text{L3}}(\text{He573})$ , obtained under the relatively undefined experimental conditions utilized in that work, show an atop signature for the acidic ( $x = 0.63$ ) support and a  $n$ -fold signature for the basic ( $x = 1.25$ ) support. The fact that these individual signatures (atop or  $n$ -fold) are detected implies that under these experimental conditions the hydrogen coverage is relatively low (no detection of weakly bonded ontop H). Therefore, the experimental conditions existing in this case must be such that the ‘strongly’ bonded hydrogen is in the atop sites for Pt particles on acid supports and in the  $n$ -fold sites on basic supports. Extrapolating the trends discussed above to small particles as shown in Figure 1 then suggest that the  $T_{\text{H}}$  and  $T_{\text{He}}$  must be similar to the  $T_{\text{vac}}$  temperatures shown in Figure 1. The effective H partial pressures during the reduction at  $T_{\text{H}}$  and evacuation at  $T_{\text{He}}$  of the LTL samples are not known. The in-situ cell was closed at some point during the cool to LN, at which point the remaining H<sub>2</sub> in the cell could adsorb. Since H<sub>2</sub> is known to

adsorb not only on the Pt, but also onto the support at low temperature (certainly at LN temperature), the effective H<sub>2</sub> partial pressure is not known. Further, the partial pressure of H<sub>2</sub> in the He desorption measurements inside the zeolite is not known, because the H<sub>2</sub> could be slow in diffusing out of the zeolite during the desorption process. Consistent with the Langmuir adsorption isotherm, the desorption temperature is highly dependent on the H<sub>2</sub> partial pressure. Thus it is difficult to correlate the temperatures  $T_{\text{H}}$  and  $T_{\text{He}}$  for the results obtained for the Pt/LTL work with the  $T_{\text{vac}}$  temperatures found in typical H<sub>2</sub> TPD data from polycrystalline Pt. This correlation can be made based on the  $\Delta\mu$  signatures obtained.

As noted above,  $T_{\text{H}}$  is a temperature somewhere below 573 K when the flowing H<sub>2</sub> was shut off (certainly under experimental conditions when weakly bonded H is not on the surface). The  $\Delta\mu$  signature indicates that the reduced Pt/LTL samples still do not have weakly bonded H present even after the cool, so apparently the existing cell H is mostly “used up” just adsorbing into the strongly bonded Pt sites and onto the support. This places  $T_{\text{H}}$  on the  $T_{\text{vac}}$  scale somewhere between 373 and 424 K. Finally,  $T_{\text{He}}$  at a temperature of 573 K in He, apparently correlates to a temperature of  $T_{\text{vac}} = 473$  K. This suggests that indeed the H pressure is somewhat higher inside the zeolite as expected.

**Confirmation of Figure 1 by H/M Experiments.** Figure 1 (right side) shows that on small particles the  $n$ -fold edge sites (the strongly bonded H) have significantly higher binding energy on basic supports compared to acidic supports. This is confirmed by standard H<sub>2</sub> chemisorption experiments performed on the Pt/LTL( $x$ ) catalysts, where the Pt particle sizes for all values of  $x$  are about the same. In Figure 10, the ratio of the strongly adsorbed H to the total adsorbed H (strong plus weak) as a function of the K/Al ratio is given. As can be seen, the relative amount of strongly adsorbed H increases with increasing basicity (K/Al ratio) of the support. As indicated by Figure 1, the ontop H is certainly part of the weakly bonded H. On acidic supports part of the weakly adsorbed hydrogen also originates from the  $n$ -fold edge sites. This fraction depends of the ionicity of the support. Therefore, the classification of the atop,  $n$ -fold and ontop sites into weakly and strongly bonded H depends strongly on the ionicity of the support. Moreover, the temperature at which hydrogen chemisorption experiments are carried out determines the origin of the sites that adsorb hydrogen “irreversibly” or “reversibly”. Preliminary hydrogen chemisorption experiments carried out at RT on an acidic Pt/H–USY catalysts show that both the amount of weakly and strongly hydrogen are smaller in comparison with a basic Pt/NaY sample. However, the average Pt particle sizes as determined with HRTEM are about the same. This would imply that the use of H/M experiments for determining the dispersion of Pt particles on supports with different ionicity or acid/base properties is questionable.

Experimentally, H/Pt ratios larger than 1 are commonly found in highly dispersed Pt in supported metal catalysts.<sup>16</sup> These high H/Pt values are also a strong indication that at high coverage hydrogen can adsorb on the  $n$ -fold sites simultaneously with very weakly bonded H in the atop sites, giving the ontop sites. In contrast, strongly bonded atop and 3-fold H to the same Pt atom does not coexist. These experimental chemisorption data in combination with the ADF calculations on a supported Pt<sub>4</sub>

cluster together with the above-discussed  $\Delta\mu$   $L_3$  difference spectra confirm that both atop,  $n$ -fold and ontop sites have to be taken into account in describing the H chemisorption process on the surface of supported Pt particles.

The transition between small and intermediate, and between intermediate and large particles, needs to be established. The transition between very small and intermediate size particles occurs when  $n$ -fold sites on the faces appear (Figure 2).<sup>12</sup> H chemisorption on the faces is weak. This means that the fraction of strongly bonded hydrogen will decrease with increasing particle size at this transition. The transition between intermediate and large particles occurs when atop H becomes delocalized. Tables 1 and 2 show that the particles on  $\text{Cl-Al}_2\text{O}_3$  are larger than those on the  $\text{K-Al}_2\text{O}_3$ . Nevertheless, the  $\Delta\mu$  line shape still shows an atop signature for  $\text{Cl-Al}_2\text{O}_3$  after evacuation at 473 K implying that delocalized hydrogen still does not exist for Pt particles with  $N = 8.8$ .

**Implications for Heterogeneous Catalysis over Supported Pt Particles.** The influence of the support ionicity on the catalytic properties of Pt particles has been investigated by our group for hydrogenolysis of neo-pentane<sup>8,9,33,34</sup> and hydrogenation of tetralin in the presence of dibenzothiophene.<sup>9</sup> Both mesoporous flat<sup>34</sup> and zeolitic supports<sup>8,9,33</sup> were used. The changes in catalytic properties of the Pt particles were related to changes in the Pt electronic structure. Our work has shown that with increasing ionicity of the support oxygen atoms: (i) the complete Pt density of states (DOS) shifts to higher energy (lower binding energy), (ii) the location of the 6s,p interstitial bonding orbital (IBO) moves from the metal–support interface to the surface of the Pt particles.<sup>8,9</sup> The ADF calculations<sup>3,10</sup> led to the understanding that the Pt sp orbitals are important for H bonding, and that the rearrangement of the Pt 6s,6p interstitial bond orbitals (IBO) instigated by the support ionicity leads to a larger Pt–H bond strength on ionic supports. The consequence of these earlier findings is that the H coverage is larger on Pt particles dispersed on ionic supports. The new results obtained in this work make clear that not only the hydrogen coverage but as a consequence also the empty Pt sites available for adsorption of reactants at high temperature catalytic reaction conditions, will strongly depend on the ionicity of the support.

The importance of hydrogen in Pt catalyzed reactions, such as those utilized in industry, has been discussed extensively in the literature. Paal and Menon<sup>35</sup> describe the role of hydrogen in industrial catalysis based on the knowledge obtained from hydrogen adsorption on single crystals. On Pt(111) crystal surfaces, only the metal 3-fold sites (fcc) are known to be important for  $\text{H}_2$  dissociation and adsorption of atomic hydrogen. The importance of hydrogen in 3-fold metal sites for catalyzing hydrocarbon reactions has been discussed since early 1980.<sup>36</sup> However, the Pt XANES  $\Delta\mu$  data and the results of the DFT calculations presented in this study show that one cannot make a simple extrapolation from single-crystal surfaces to small particles, since on small and intermediate size Pt particles (sizes

smaller than 20–25 Å) H in ontop and atop sites can also play an important role.

The new insight obtained in this work that the ionicity of the support determines both the hydrogen coverage and the type of empty site available for adsorption of reactants has large implications for Pt catalyzed reactions, such as hydrogenolysis of alkanes and hydrogenation of aromatic alkenes (benzene) or oxygenated aromatic alkenes (benzaldehyde, cinnamaldehyde). The conversion rate for hydrogenolysis of alkanes is several orders of magnitude higher when the Pt particles are dispersed on covalent supports (acidic, with electron poor O atoms). A detailed analysis<sup>3</sup> of the kinetic data for neopentane ( $\text{C}-(\text{CH}_3)_4$ ) hydrogenolysis showed that the H coverage directly affects the neopentane–Pt bond strength through lateral interactions (i.e., via a Frumkin isotherm effect), and thereby changes the activation energy for the reaction. The change in H coverage is believed to be the most responsible for the observed change in reactivity.

Preliminary results<sup>37</sup> for hydrogenation of benzene and other oxygenated alkenes catalyzed by Pt on oxidic supports (including those with different ionicities) and on carbon supports (with different amounts of oxygen containing groups) show much lower apparent activation energies in comparison to hydrogenolysis reactions. The changing kinetics and order in reactants can now be explained by assuming that the alkene reactant is not directly adsorbed on the Pt particles but is in pre-equilibrium with the support. The production of mobile atomic hydrogen (from  $\text{H}_2$  dissociated on Pt) is proposed to be the rate-determining step. The properties of the support (such as acidity) control which type of empty Pt surface site is available to produce the mobile H. The activation energy of the reaction is then determined by the reaction enthalpy for the dissociation of  $\text{H}_2$  on the available empty Pt surface sites. A full explanation of the influence of the support properties on the kinetics of Pt catalyzed hydrogenation reactions will be given in forthcoming papers.<sup>37</sup>

Understanding the fundamental mechanism of the metal–support interaction opens the possibility for the synthesis of tailor-made catalysts. As already discussed in an earlier paper<sup>3</sup> the dependence of the position in energy of the Pt d-band density of states on the ionicity of the support oxygen atoms can be utilized to optimize the reactivity of catalytic intermediates with the Pt surface. For instance, a catalytic reaction with catalytic intermediates that need metal surface valence orbitals with electron acceptor or donor properties, requires a metal particles to be prepared on a support with oxygen atoms having electron poor (covalent or acidic) or electron rich (ionic or basic) support oxygen atoms. This work reveals the role of the support in influencing the adsorption properties of adsorbates both in terms of coverage and adsorption site. For instance, a catalytic reaction with catalytic intermediates that require a specific metal surface site suggests that a specific support has to be used. For zeolitic supports, the composition can be tuned by introducing protons, changing cations, Si/Al ratio or by steaming (the latter leads to the presence of extraframework Al). For instance, a catalyst for aromatic saturation can be made sulfur tolerant (high catalytic activity in the presence of sulfur) by making the support acidic, by increasing the polarization power of the charge compensating

(33) Koningsberger, D. C.; de Graaf, J.; Mojet, B. L.; Ramaker, D. E.; Miller, J. T. *Appl. Catal. A* **2000**, *191*, 205–220.

(34) Koningsberger, D. C.; Oudenhuijzen, M. K.; Ramaker, D. E.; Miller, J. T. *Stud. Surf. Sci. Catal.*, 12<sup>th</sup> Int. Congr. on Catal., Eds. Corma, A., Melo, F. V., Mendioroz, S., and Fierro, J. L. G., Elsevier: **2000**, *130A*, 317–322.

(35) *Hydrogen Effects in Catalysis: Fundamentals and Practical Applications*; Paal, Z., Menon, P. G., Ed.; Dekker: New York, 1988.

(36) Paal, Z. *Advances in Catalysis*, **1980**, *29*, 273–288.

(37) Stakheev, A. Yu.; Zhang, Y.; Ivanov, A. V.; Baeva, G. N.; de Jong, K. P.; Ramaker, D. E.; Koningsberger, D. C., to be published.

cations, by decreasing the Si/Al ratio and by introducing extraframework Al.<sup>9</sup> Although much progress has been made as suggested above, more research is needed to fully explore the possibilities for tuning the catalytic properties of a supported metal particle by changing the properties of the support.

## Conclusions

Hydrogen adsorption on Pt/Cl–Al<sub>2</sub>O<sub>3</sub> and Pt/K–Al<sub>2</sub>O<sub>3</sub>, along with Pt/LTL(*x*) has been studied utilizing Pt L<sub>2,3</sub> XANES data. Both the effects of particle size and support ionicity or acid/base properties were investigated. The preferred H absorption site can be ascertained from the signature of the Pt  $\Delta\mu_{L3}$  XANES difference spectra: L<sub>3</sub> edge measured in the presence of chemisorbed hydrogen minus L<sub>3</sub> edge taken in a vacuum. Three different hydrogen adsorption sites can be distinguished: atop, *n*-fold (*n* = 2 or 3) and ontop. The hydrogen coverage, the temperature of evacuation and the support ionicity or acid/base properties determine which sites are detected with the  $\Delta\mu_{L3}$  difference technique.

A full understanding of the experimental results is obtained with density functional calculations using the ADF code. The theoretical calculations show that the Pt–H bond strength for an atop site is higher for Pt on ionic (basic) supports. Moreover, the ADF results demonstrate that with increasing hydrogen coverage the atop H becomes unstable causing it to move to an *n*-fold site.

Combining the results of the  $\Delta\mu_{L3}$  difference technique with the density functional calculations reveals that the first hydrogen

adsorbs in the atop site. With increasing hydrogen pressure or decreasing temperature, the *n*-fold sites become populated at the expense of the atop sites. Finally, hydrogen can adsorb very weakly in ontop site, defined as an atop Pt site, for which this Pt already has a stronger bond to a H atom in a *n*-fold site. The results show that the total coverage and the fraction of strongly bonded hydrogen is higher for Pt on ionic/basic supports.

The results obtained in this work imply that both the hydrogen coverage and the type of Pt surface sites available for dissociation of hydrogen and adsorption of reactants existing under high temperature catalytic reaction conditions, strongly depends on the ionicity of the support. Since hydrogen is involved in many industrial type Pt catalyzed reactions, it is very likely that the results of this study are relevant for the design of tailor-made Pt catalysts.

**Acknowledgment.** The authors would like to acknowledge the scientific staff of station 9.2 of the SRS (Daresbury, UK), BM29 of the ESRF (Grenoble, France) and beamline X1.1 of Hasylab (Hamburg, Germany). Also the European Union program for Large Scale Facilities (Contract No. ERBFMGECT-950059) is acknowledges for financial support.

**Supporting Information Available:** Experimental data for Pt particles on covalent supports, types of hydrogen adsorption site on the surface of the Pt particles. This material is available free of charge via the Internet at <http://pubs.acs.org>.

JA045286C